Pergamon

European Journal of Cancer Vol. 30A, No. 7, pp. 994–1002, 1994
Copyright © 1994 Elsevier Science Ltd
Printed in Great Britain. All rights reserved
0959–8049/94 $7.00+0.00

0959-8049(94)E0146-U

Hypersomy of Chromosome 15 With Retrovirally Rearranged c-*myc*, Loss of Germline c-*myc* and IgK/c-*myc* Juxtaposition in a Macrophage–Monocytic Tumour Line

S. Imreh, Y. Wang, C.K. Panda, M. Babonits, H. Axelson, S. Silva, A. Szeles, F. Wiener and G. Klein

From a lymphoid tumour induced by 7,12-dimethylbenz-[a]-anthracene (DMBA) + methyl-*N*-nitrose-*N*-urea (MNU) in an [AKR Rb(6.15) × CBAT6T6]F1 mouse, a macrophage– monocyte line (KT-10) was isolated. Following ethyl methanesulfonate (EMS) treatment, a bromodeoxyuridine (BUdR) resistant subline was selected. Serial propagation of this line *in vitro* in the presence of BUdR (28 months) with periodic cytogenetic and molecular examinations, has led to the definition of four successive stages. During stage I, the cells were trisomic for chromosome 15. They contained Rb(6.15) and Rb(del6.15) of AKR and T(14;15) of CBA origin. Southern blotting showed the presence of both germline (G) and rearranged (R) c-*myc*. At stage II, Rb(del6.15) has duplicated. Both Rb(6.15) and T(14;15) persisted together with G-*myc* and R-*myc*. In stage III, the CBA-derived T(14;15) was lost, in parallel with G-*myc*. At this stage, a Dic.In(6.15) was detected. One of its arms was cytogenetically identical with the long arm of In(6.15) in the variant IgK/*myc* translocations. This chromosome carried R-*myc* and IgK in juxtaposition, as indicated by comigration on pulsed field electrophoresis (PFGE). At stage IV, the R-*myc* carrying AKR-derived chromsome 15s were present in six copies. Possible relationships between the increasing R/G *myc* ratio and changed growth characteristics *in vivo* and *in vitro* are discussed.

Key words: chromosome aberrations, C-*myc* genes, immunoglobulin kappa chain, lymphoma, macrophages, oncogenes, retroviruses

Eur J Cancer, Vol. 30A, No. 7, pp. 994–1002, 1994

INTRODUCTION

TRISOMY 15 is the most frequent non-random chromosome anomaly in murine T-cell lymphomas, irrespectively of aetiology. In the virally induced T-cell lymphomas, retroviral genomes are frequently inserted in the locality of the c-*myc* or the linked *pvt*-1 gene [1–4].

Three murine T-cell lymphomas with trisomy 15 and retroviral insertion in the c-*myc* region have been investigated previously. TIKAUT is a 6-thyoguanine (TG)+ ouabain-resistant subline of the AKR-derived 15-trisomic T-cell lymphoma TKA. TKA contained a mink cell focus-forming (MCF) type retroviral insertion in inverse transcriptional orientation, 1.3 kb 5′ of c-*myc* (R-*myc*), and also the germline c-*myc* (G-*myc*) (R:G ratio = 2:1). After *in vitro* cultivation and selection for TG and ouabain resistance, the TIKAUT variant was still trisomic for chromosome 15, but the germline c-*myc* was no longer present. This has led to the conclusion that the duplicated R-*myc*-carrying chromosome has duplicated once again, while its G-*myc* homologue was lost (R:G ratio = 3:0) [5–8]. The c-*myc* mRNA level was 5-fold higher in TIKAUT than in T-cell lymphomas without R-*myc* [8]. Another AKR-derived T-cell lymphoma, the MCF247 virus-induced MCF-B, was examined after mutation and selection for BUdR and ouabain resistance. It was trisomic for chromosome 15 with an R:G ratio of 2:1 [9, 10]. Another lymphoma of the same category, YAC-1, and its TG and ouabain-resistant derivative YACUT carried a retroviral insertion in the *pvt*-1 region (at least 72 kb downstream of c-*myc*), known as the preferred breakage site of the variant IgK/*myc* translocations [11].

The R-*myc*-carrying lymphomas mentioned above were fused to diploid fibroblasts and/or lymphocytes. Compared with the normal parent, high malignant segregants had increased tumour, chromosome 15 ratio in contrast to their low malignant counterparts [5, 10, 12]. The dominance of the R-*myc*-carrying leukaemia-derived chromosome 15 over its G-*myc*-carrying, normal parent-derived counterpart in the high tumorigenic hybrids suggested that this asymmetry contributed to the growth advantage of the cells *in vivo*.

We describe a serially cultivated macrophage–monocyte line that has been derived from a primary lymphoma, induced in a DMBA (7, 12-Dimethylbenz-[a]-anthracene) + MNU (methyl-*N*-nitroso-*N*-urea) treated [AKR Rb(6.15) × CBAT6T6]F1

Correspondence to S. Imreh.
The authors are at the Department of Tumor Biology, Karolinska Institute, Box 60400, S-10401 Stockholm, Sweden. C. K. Panda is presently at Chittaranjan National Cancer Institute, 37 S.P. Mukherjee Road, Calcutta 700 026, India.
Received 18 Nov. 1993; accepted 25 Jan. 1994.

mouse by chemical carcinogen treatment. Designated as KT-10, the line contained rearranged (R) and a germline (G) c-*myc*-carrying chromosome 15 in a ratio of 2:1. In the course of serial *in vitro* passages, the number of R-*myc*-carrying chromosome 15s increased from two to six copies, whereas the G-*myc*-carrying chromosome was lost. Also, a pericentric inversion occurred in a Rb(6.15) chromosome, similar to the IgK/*myc* variant translocation seen in mouse plasmacytomas, induced in (BALB/c × AKR6.15)F2 mice with the Robertsonian fusion Rb(6.15) chromosome [13]. Pulsed field electrophoresis (PFGE) and comigration studies have confirmed the juxtaposition of IgK and c-*myc* at this stage.

MATERIALS AND METHODS

Mice and tumour induction

F1 hybrid mice were produced by crossing AKR (Rb(6.15)Ald1 mice, known as AKR6.15 [14], with CBA T(14;15)6Ca mice, known as CBAT6T6 [15]. The parental origin of each chromosome 15 could be readily identified in the F1 hybrids. Newborns were injected intraperitoneally (i.p.) with 0.1 ml phosphate buffered saline (PBS) containing 0.05 mg MNU. One milligramme of DMBA dissolved in 0.1 ml polyethylene glycol (PEG mw 400) was administered through a stomach tube four times at monthly intervals, starting at 4 weeks of age. The donor of the KT-10 line developed lymphoma after 124 days. Smears prepared from lymph nodes were stained with May–Grünwald–Giemsa stain.

Origin and history of the KT-10 line

The origin and passage history of the KT-10 line is summarised below:

Stage 0 (0–2 *months*). The KT-10 tumour appeared in an [AKR Rb(6.15) × CBAT6T6]F1 mouse, treated with DMBA and MNU, after a latency period of 124 days. Conventional Giemsa staining showed 39 chromosomes, one T6 marker for CBA and two biarmed Rb(6.15) from the AKR parent. The tumour was thus trisomic for chromosome 15. Mononuclear cells were separated from an enlarged mesenterial lymph node by gradient density centrifugation on Ficoll. The cells were explanted on the feeder layer of the original organ in RPMI medium supplemented with 10% fetal calf serum (FCS). After a few passages, non-adherent cells were frozen for more than a year.

Stage I (7 *months*). Seven slowly growing adherent clones were isolated. One clone that had the same karyotype as stage 0, designated KT-10, was propagated further in RPMI medium supplemented with 10% FCS.

Stage II (6 *months*). The line was mutagenised by EMS (100 μg/ml) followed by stepwise selection on bromodeoxyuridine (BUdR) (up to 50 mg/ml).

Stage III (6 *months*). Second mutagenisation in EMS followed by BUdR + verapamil (5 μg/ml) + H33258 (40 μg/ml) + light selection [16, 17]. A HAT sensitive clone was further propagated *in vitro*.

Stage IV (7 *months*). Ten *in vivo* (i.v.) passages in syngeneic (AKR×CBA)F1 mice. The line was carried further in Iscove's medium containing BUdR before karyotpying.

Surface marker analyses and phagocytic tests

Cells grown on multichamber slides were analysed in stages I and IV for the expression of T- and B-cell surface antigens. The antibodies included FITC (fluorescein isothiocyanate) conjugated, anti-Thy-1, rabbit anti-mouse-Ig and B220. As second control antibody, FITC-conjugated rabbit anti-rat Ig was used. Macrophage surface markers were determined by FITC-conjugated anti-macrophage–granulocyte Mac-1 and Mac-2 monoclonal- and F4/80 macrophage-specific antibodies. The phagocytic test was performed by exposing cells growing on coverslips to 2.8-μm sized plastic beads and to iron powder. The positive and negative controls included the AKR-derived, T-cell line TIKAUT [5], the mouse mammary carcinoma line, SHG [18], AKR-derived splenocytes and macrophages.

Cytogenetic analysis

Conventional G and C and high resolution G bandings on synchronised cells were performed as described [19–21]. Chromosomes were identified according to the criteria specified by the Committee of Standardised Genetic Nomenclature for Mice [22]. At least 10 G-banded mitoses were karyotyped in each stage. Fluorescent *in situ* hybridisation (FISH) with a biotin-labelled mouse minor satellite probe [23] was carried out as previously described [24].

Population doubling time

Cells were plated at low density. Mean cell numbers of individually marked clones were counted daily under an inverted microscope and plotted against time. Growth rate was calculated from the steepest part (between days 2–5) of the curve.

Tumorigenicity

Take incidences (number of tumours developed per inoculated mouse) were evaluated in stages I and IV. One hundred to 10^7 cells were inoculated into SCID mice. Animals that failed to develop tumours within an observation period of 2 months were considered negative.

Southern, PFGE and northern analysis

Southern blotting was performed after *Eco*RI and *Kpn* I digestion. Probes utilised were c-*myc* exon 1, 369 bp Hind III/Xhol fragment subcloned from Pm c-*myc* 54 [25]; c-*myc* exon 3, 369 bp Pvu II/Xhol fragment subcloned from Pm C-*myc* 54 [25]; AKV U3 LTR, 250 bp Pst I fragment released from AKV MCp15E/U3 LTR [3]; pvt-1e, 0.7 kb *Eco*RI fragment [26] and a 2-kb *Bam*HI/*Eco*RI fragment of a JH probe [27]. PFGE analysis was performed to assess the relationship of the C-*myc* to IgK. Sal I digested DNA was probed with : c-*myc* exon 1 and c-*myc* exon 3 [25]; *pvt*-1a and *pvt*-1e [26]; IgK : 3.1 kb *Bam*HI/*Hind* III fragment containing enhancer and Ck [26]. C-*myc* mRNA and IgK expression was assessed by northern blotting as described [27].

RESULTS

Cytology

The KT-10 tumour presented with splenomegaly and generalised enlargement of peripheral and mesenteric lymph nodes, but without thymic involvement. Moderately sized cells with large round to oval nuclei, prominent nucleoli and finely dispersed chromatin were separated on Ficoll from a mesenteric lymph node. The nucleus was surrounded by a tiny rim of basophilic cytoplasm. Small lymphocytes and macrophages were interspersed between the lymphoblastoid cells. Histologically, it was diagnosed as a diffuse lymphoblastoid lymphoma.

Figure 1 and Table 1 summarise the surface marker, cytogenetic and c-*myc* status of the KT-10 cell line at stages I–IV.

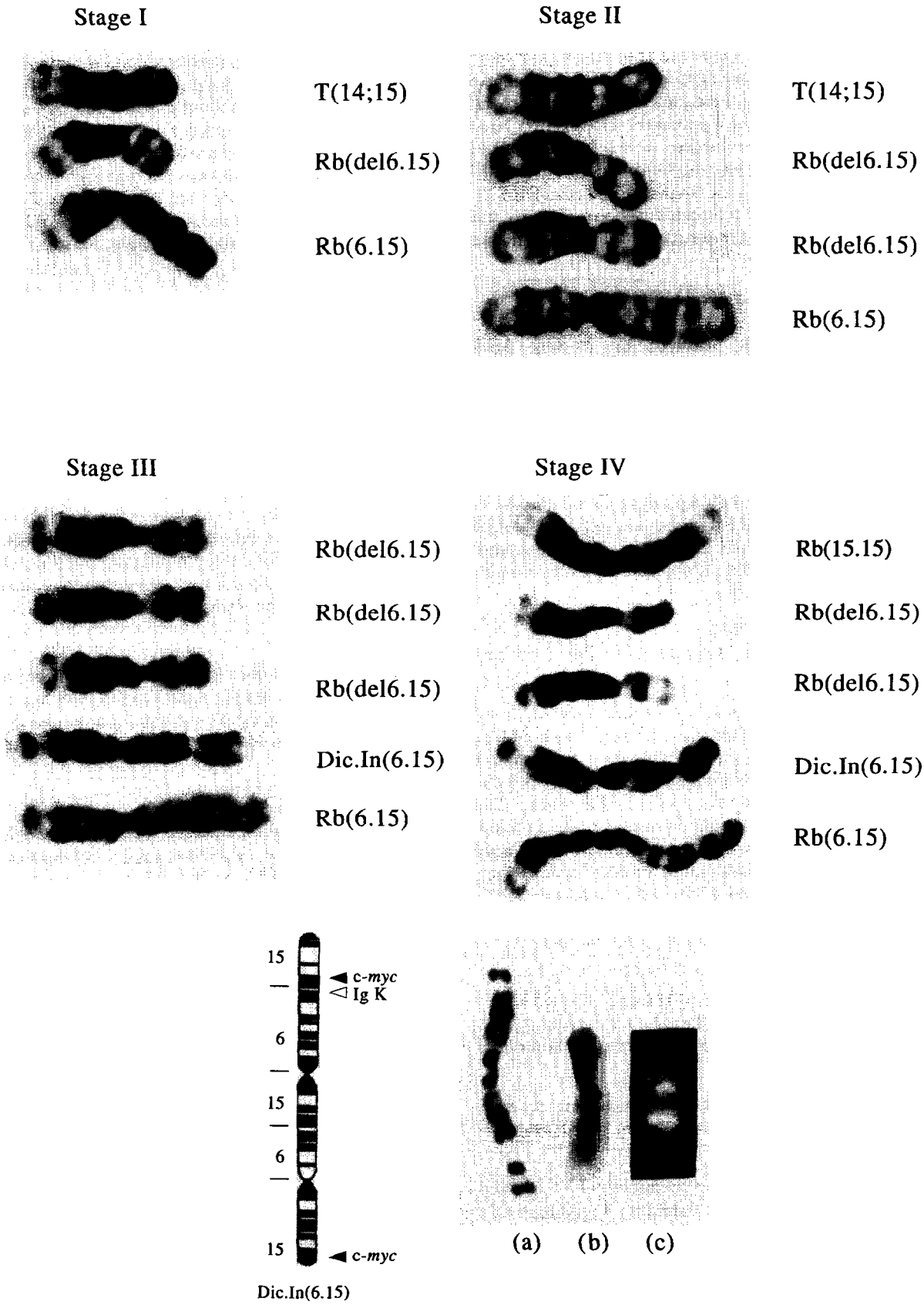

Figure 1. Chromosome 15s in the four stages of KT-10 (G-banding).Dic.In(6.15) shown on high resolution idiogram was analysed by (a) high resolution G-banding. The longer free arm is identical with the corresponding arm in the In(6.15) of BALB/c6.15 plasmacytomas. (b) C-banding and (c) FISH (with a kinetochore specific mouse minor satellite probe) showing the presence of two centromeres.

Table 1. Cytogenetic and molecular characterisation of the four KT-10 stages

Stage	CBA T(14;15)	AKR Rb(6.15)	C-*myc**	Notes
I	1	2	G+R	Rb(del6.15) one copy
II	1	3	G+R	Rb(del5.15) two copies
III	0	5	R	Dic.In(6.15) Rb(del6.15) three copies
IV	0	6	R	Dic.In(6.15)Rb(del6.15) two copies Rb(15.15) one copy

G, germline c-*myc*; R, rearranged c-*myc*.

Surface marker analysis

The *in vitro* explanted tumour cells grew initially in suspension and expressed Thy-1. During the establishment of a permanent line, the lymphoblastoid cells disappeared. Adherent cells continued to grow and were cloned. Only the latter entered the present study. In the continuation and throughout the stages I–IV, the cells had an exclusively macrophage–monocyte-like appearance, corroborated by the expression of Mac-I, Mac-II, F 4/80 surface markers, phagocytosis, trypsin-resistant adherence and cell morphology.

Cytogenetic analysis

The cytogenetic analysis defined four stages during the serial culture of macrophage–monocyte line KT-10. Stage I: trisomy 15; the AKR-derived Rb(6.15) was duplicated. However, a proximal segment of chromosome 6 (A2-C3/D) was lost, generating Rb(del6.15). The CBA-derived T(14;15) chromosome was present in a single copy in all mitoses. Stage II: the AKR-derived chromosome 15 copies increased to a mean of 3.3 by the duplication of Rb(del6.15). T(14;15) persisted. Stage III: the CBA-derived T(14;15) disappeared. The AKR-derived chromosome 15 copy number was 5.1. Rb(del6.15) trebled and a rearranged dicentric and inverted Rb(6.15) chromosome, denoted Dic.In(6.15), emerged in nine out of 10 mitoses. Stage IV: the mean number of chromosome 15 copies increased to 5.7. One Rb(15.15) isochromosome appeared in all mitoses, but 2.9 Rb(del6.15) and one Dic.In(6.15) persisted. The dicentric nature of Dic.In(6.15) was proved by C-banding and FISH. High resolution banding suggested breakpoints at 15D2/3 and 6C2 leading to a pericentric inversion (Figure 1).

Southern analyses

Southern hybridisations (Figure 2a) with c-*myc* exon 1 probe to the *Eco* RI digested DNA revealed rearranged band of 30 kb in all four stages. DNA digested with KpnI, hybridised with exon 3 probe showed a 6.3 kb band in all stages (Figure 2e). The 21 and 11 kb germ line bands were present only in stages I and II (Figures 2a,e). Hybridisation of the KpnI filter with the c-*myc* exon 1 probe exposed two rearranged bands (6.3 and 3.7 kb). This means that novel KpnI sites were generated in the region defined by exon 1 probe, suggesting that a fragment containing KpnI sites was probably inserted into this region. To test this possibility, an AKvLTRU3 specific probe was used to hybridise with the same KpnI filter. As can be seen in Figure 3c,d only the 3.7 kb but not the 6.3 kb fragment hybridised with both AKvLTRU3 and c-*myc* exon 1 probes. Because KpnI cuts only in the U5 domains of the LTRs, hybridisation of the 3.7 kb fragment with both the AKvLTRU3 and exon 1 indicates that the provirus and c-*myc* are in the same transcription orientation (Figure 2g). Hybridisation of the KpnI digested DNA with *pvt*-1 probe showed that this locus was in germline (Figure 2f). Hybridisation of *Eco*RI-digested DNA with a JH probe on *Eco*RI-digested DNA showed the loss of 6.2 germline fragment and the presence of two rearranged fragments of 3.5 and 2.3 kb size (Figure 4). This was interpreted to mean that both alleles had undergone V(D)J recombination. The same pattern was present in all four stages.

PFGE

PFGE was performed to examine whether the Dic.In(6.15) chromosome (Figure 1) carries c-*myc* and IgK in juxtaposition as suggested by the cytogenetic picture.

Figure 3a shows the hybridisation of Sal I-digested KT-10 stage II, KT-10 stage III, CCE DNA with the IgK probe. The same two germline IgK bands, 83 and 165 kb in size were found as in the control CCE (mouse embryonic stem cell line with hypomethylated DNA, see [28]). In stage III DNA, three IgK hybridising fragments were detected (135 kb germline, 225 and 260 rearranged). When this filter was stripped and rehybridised with *myc* 1.1, a *myc* hybridising band of 260 was found to comigrate with the rearranged IgK. The germline hybridising band of 90 kb found in CCE was missing from KT-10 stage III.

In a second experiment, shown in Figure 3b, stage IV DNA cut with Sal I gave rise to the same *myc* hybridising rearranged bands of 260 kb, as found in stage III. A rearranged 125 kb band occurred most probably due to a different methylation pattern. Mouse spleen used as germline control yielded the same 135 kb germline band as found in CCE in the first experiment. The 83 kb germline kappa band from the spleen control was missing, probably due to a difference in methylation.

When the same filters were rehybridised with the *pvt*-1b probe, no comigrating fragments were seen (data not shown). Ordinary Southern hybridisation showed no rearrangement at the *pvt*-1b and *pvt*-1e loci. This indicates a juxtaposition of the 5′ region of IgK (with the molecular breakpoint either in the V-kappa or 5′ V-kappa) to the 3′ region of c-*myc*, between exon 3 and *pvt*-1. The absence at stage III of the 125 kb rearranged c-*myc* band found at stage IV might be due to differential methylation of the 3′ *myc* locus.

The 260 kb c-*myc*/IgK comigrating fragment was due to the partial digestion of Sal-I site located 5′ of the IgK locus. The 225 kb rearranged IgK fragment was probably generated by physiological rearrangement of the IgK locus.

Northern analyses

As shown in Figure 5 c-*myc* was highly expressed in stage I and stage IV cells. The transcripts differed in size from the TEPC Hi-6 sample used as a prototype IgK/*myc* translocation carrier. This difference may have been due to the fact that part or all of the KT-10 transcripts originated from the retrovirally rearranged c-*myc* allele. There was no evidence of kappa constant region expressions.

Growth and tumorigenicity

The cell number in individual clones increased faster in stage IV than in stage I. The average doubling time was 41.0 h in stage I and 23.1 h in stage IV.

Table 2 shows the results of the tumorigenicity tests in SCID mice. Inocula between 10^3 and 10^6 of KT-10 stage I cells failed to grow in 22 SCID mice. Inocula between 10^3 and 10^7 of stage IV cells grew in 12 of 18 inoculated SCID mice (67%).

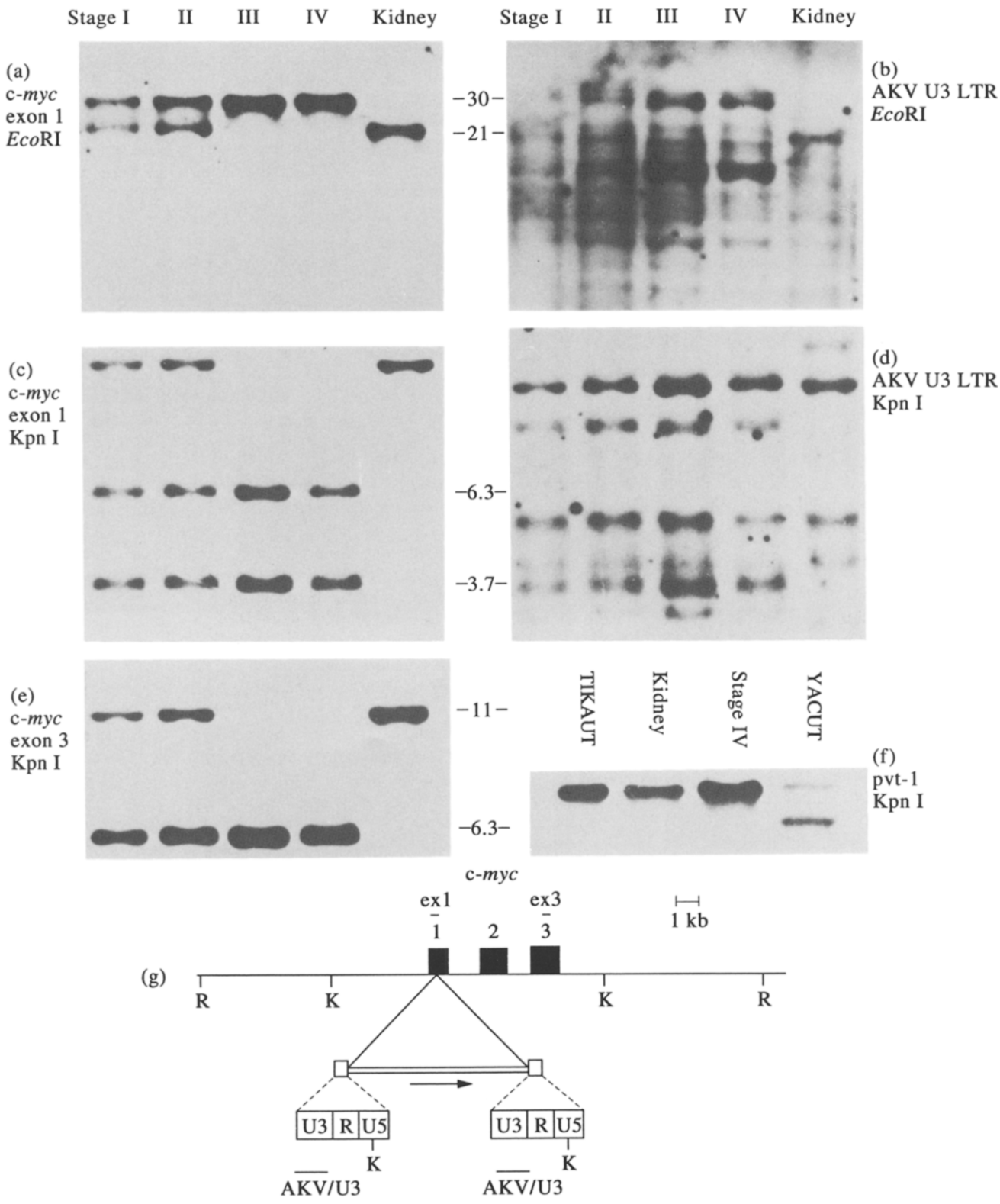

Figure 2. Southern blots of KT-10 stages I–IV. (a) Exon 1 probe hybridisation of *Eco*RI-digested DNA shows one rearranged c-*myc* band and loss of germline c-*myc* at stages III–IV. (b) R-*myc* comigrates with retroviral LTR (*Eco*RI digestion). (c, d) Exon 1 probe hybridisation after Kpn I digestion shows two R-*myc* bands. The 3.7 kb band comigrate with AKV U3 LTR. (e) C-*myc* exon 3 hybridisation on Kpn I-digested DNA shows only one R-*myc* band of 6.3 kb. (f) Hybridisation with *pvt*-1 probe. Note that the germline configuration at stage IV is the same as in TIKAUT and normal kidney lanes. YACUT shows the previously known *pvt*-1 rearrangement [11]. (g) Map of the c-*myc* region with retroviral insertion in exon 1. (Code for restriction endonucleases: K, Kpnl; R, *Eco*RI; code for probes: ex1, c-*myc* exon 1probe; ex3, c-*myc* exon 3 probe; AKV/U3, AKV U3 LTR probe see Materials and Methods for details.) The arrow indicates transcriptional orientation.

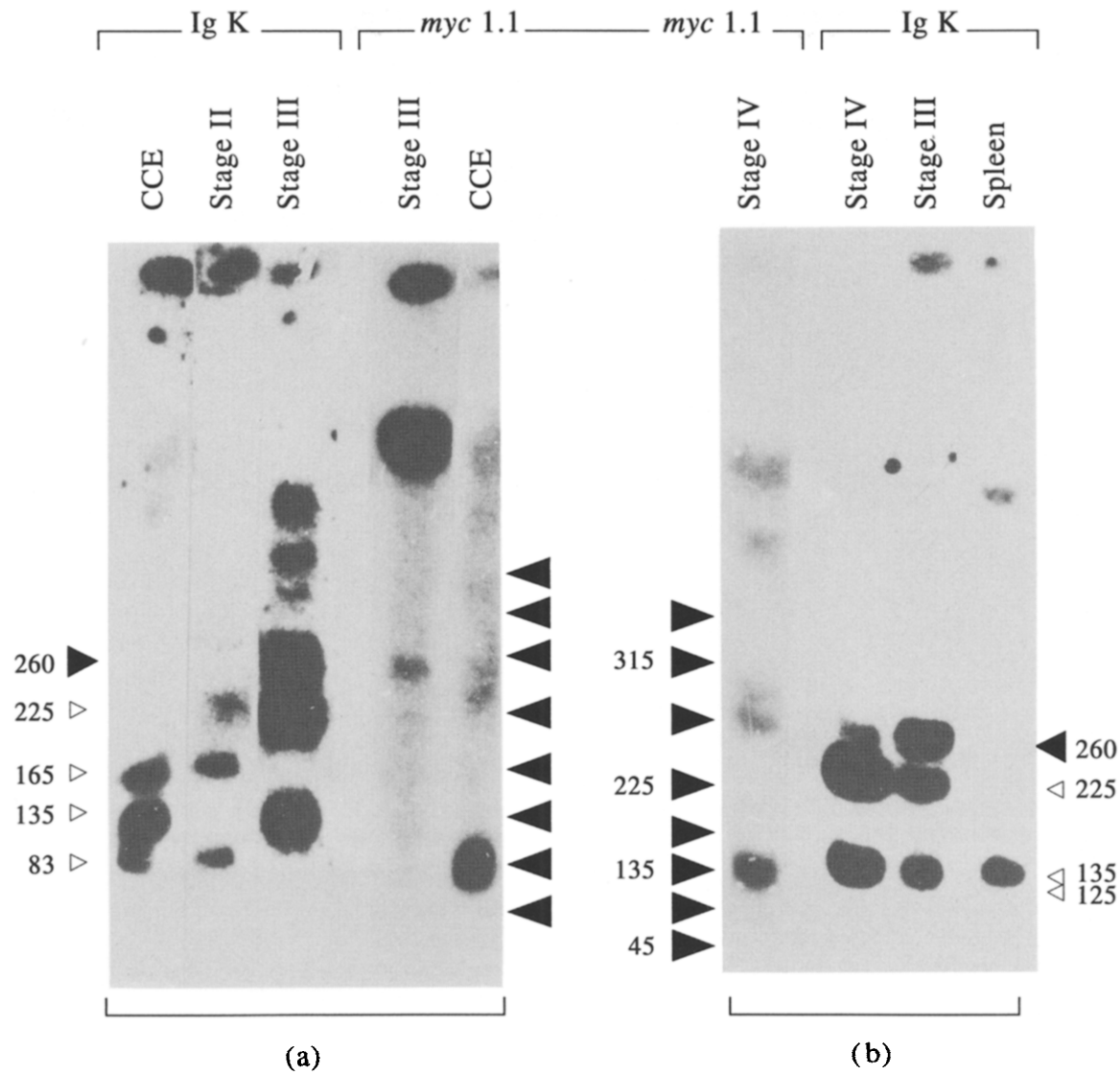

Figure 3. PFGE Southern blot analysis of KT-10 DNA at different stages. The DNA was digested with Sal I. The same Southern blots were hybridised sequentially with IgK constant region and MYC 1.1 probes. Size marker: lambda phage DNA multimers as indicated between the two panels. Hybridising bands are indicated by open arrows. Large solid arrows indicate comigrating *myc*/IgK bands on both panels a and b.

DISCUSSION

Hypersomy of the R-*myc*-carrying and elimination of the G-*myc*-carrying chromosome 15 were the most notable cytogenetic changes during serial *in vitro* propagation of the KT-10 line. The following findings appear to be of particular interest:

(a) KT-10 originated as a lymphoma, but the derived cell line was adherent, with macrophage–monocyte characteristics during its entire subsequent history. Molecular data are not available from the original primary tumour. The adherent line was still trisomic for chromosome 15 as the original *in vivo* tumour, and carried R-*myc*, already at stage I. The non-productive rearrangement of both IgH loci at all four stages and the IgK/c-*myc* translocation at stage III and IV indicate that the tumour may have originated from an early pro- or pre-B cell. The commitment to a macrophage–monocyte-like phenotype may have occurred after explanation. Hara and colleagues [29] have derived an adherent, macrophage-like subline from a pre-B line and B-cell precursors have been switched to monocytes by transfecting them with certain oncogenes and growth factors [30].

(b) The R-*myc* was generated by the insertion of an endogenous retrovirus into the first exon of c-*myc*, downstream of the P1 and P2 promoters. Retroviral insertions occur frequently in the locality of c-*myc*, usually upstream of the gene, although occasional downstream insertions have been found [31]. Insertions within exon 1 have been described in four of 33 MoMuLV-induced leukaemias studied by Selten and colleagues (cited by [32]). Two of them carried the insertion in the same orientation as c-*myc*, like in KT-10, and maintained both LTRs. R-*myc* has been found in approximately 10% of all viral-induced murine lymphomas [8, 9]. Chemically or X-ray-induced T-lymphomas showed no rearranged c-*myc* on Southern analysis [32].

(c) The R-*myc*-carrying chromosome 15 became hypersomic in the course of serial *in vitro* passage. This was accompanied by some concomitant changes, starting with the loss of a proximal A2-C3/D segment of chromosome 6.

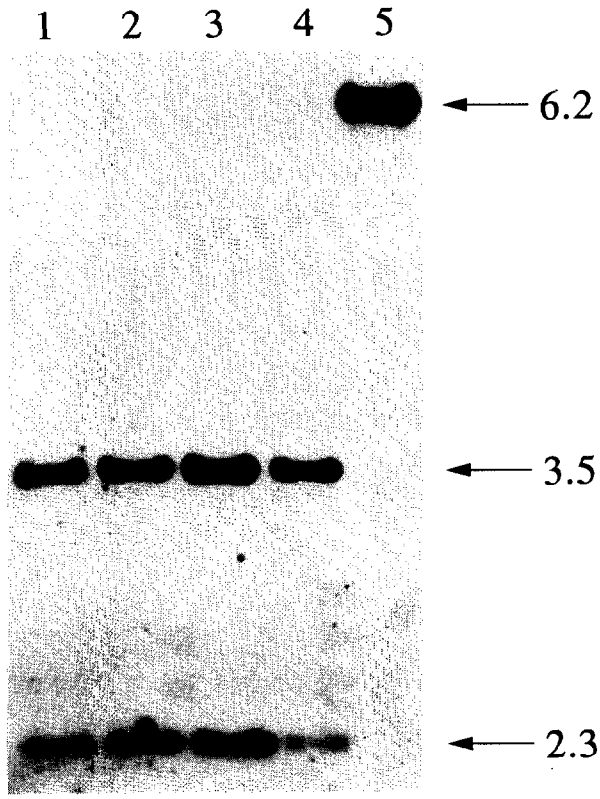

Figure 4. Southern analysis of *Eco*RI-digested DNA of the four KT-10 stages (lanes 1, 2, 3, 4) and AKR kidney control (lane 5) shows rearrangement of the JH region in all KT-10 stages. Numbers adjacent to the arrows denote the size of the band in kb.

The derived Rb(del6.15) product was duplicated twice in stages II and III. Rb(15.15) appeared at stage IV, probably by centric fission of Rb(6.15) or Rb(del6.15), followed by the duplication of the fissioned acrocentric 15 and the loss of the entire or the deleted chromosome 6, as described in spontaneous AKR lymphomas [33].

The longer free arm of Dic.In(6.15), that appeared in stage III, was morphologically undistinguishable from the long arm of In(6.15) in the variant IgK/*myc* translocations, that we have previously detected in mouse plasmacytomas, induced in (BALB/c × AKR6.15)F2 mice [13, 34]. Since the long arm of Dic.In(6.15) in KT-10 was part of a dicentric chromosome, it may be presumed that the Rb(6.15) was duplicated between the stages II and III, but the duplicated homologue underwent pericentric inversion with breakpoints 6C2 and 15D2/3. The In(6.15) derivative and Rb(del6.15) may have entered into a reciprocal translocation (breakpoints 15B3, 6E and 15D2/3), resulting Dic.In(6.15) (Figure 4). PFGE analysis detected comigrating R-*myc*/IgK fragments, indicating juxtaposition of the two genes, consistent with a variant kappa/myc translocation. The breakpoint on chromosome 15 was found between *myc* exon 3 and *pvt*-1. On chromosome 6, the breakpoint was either in V_k or 5′ of V_k, leaving the kappa

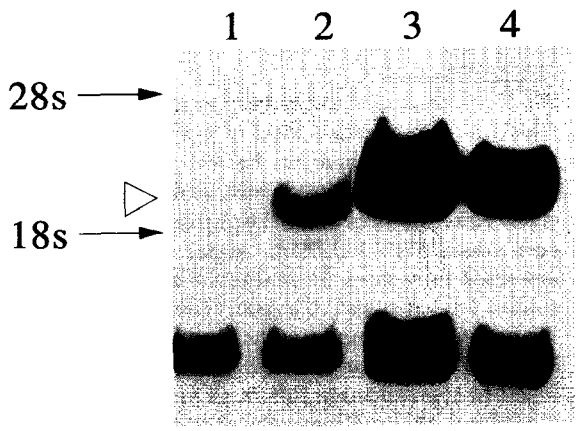

Figure 5. Northern blot analysis. Lane 1: mouse kidney control RNA, lane 2: mouse plasmacytoma TEPC Hi-6 RNA, lane 3: KT-10 stage IV RNA, lane 4: KT-10 stage I. Blot was probed with c-*myc* probes (upper signals) and control housekeeping gene GAPDH (lower signal). Arrows indicate 18s and 28s ribosomal ARNs. Open arrow position of the weak kidney signal.

Table 2. Tumorigenicity of KT-10 stage I cells compared with stage IV cells. Take incidences (take inc.) evaluated after an observation period of 2 months

Cell no.	Stage I Take inc.	Stage IV Take inc.
10^2	nd	0/2
10^3	0/4	3/5
10^4	0/6	0/2
10^5	0/7	3/5
10^6	0/5	2/2
10^7	2/4	4/4
Totals	2/26	12/20

nd, not determined.

enhancer region intact (VJk in germline configuration, data not shown). In the T(6;15)-carrying MPC variants, the kappa locus is usually juxtaposed to the *pvt*-1 region [31]. In a recently discovered IgL/*myc* (15;16) translocation, the breakpoint was between *myc* and *pvt*-1, however [27].

(d) Loss of the G-*myc*-carrying chromosome 15 at stage III may be coincidental or selective. The latter possibility is suggested by analogous observations on three different T-cell lymphomas, TIKAUT, MCF-B and YACUT, as mentioned in the Introduction. Serial propagation of these tumours was accompanied by duplication and even trebling of the R-*myc*-carrying and loss of G-*myc*-carrying chromosome. It is also in line with the amplification of the leukaemia-derived, R-*myc*-carrying chromosome, and the disappearance of the normal parent derived G-*myc* carrier chromosome in high tumorigenic lymphoma/fibroblast hybrids.

The microevolution of the KT-10 line *in vitro* is interesting for several reasons. Although it is a chemically induced lymphoma, it carries an endogenous (AKv type) ecotropic virus inserted within exon 1 of c-*myc*. It has a macrophage–monocyte phenotype, but both of its IgH alleles are non-productively rearranged. Moreover, it has acquired a kappa/*myc* translocation, previously only found in B-cell derived tumours. IgK/*myc* is the most frequent variant (light chain involving) translocation in MPC, and it is already present in the primary tumour. KT-10 provides the first example where an Ig/*myc* translocation appears during *in vitro* culture. Repeated mutagenisation with EMS, followed by BUdR selection, may or may not have contributed to this development. It is also noteworthy that the R-*myc* locus participating in this translocation has been apparently doubly activated by retroviral insertion in exon 1, and by the kappa enhancer located downstreams of the gene. The translocation may have provided the cell with an additional selective advantage, compared to the effect of retroviral insertion itself [32]. Probably, juxtaposition of Ig sequences provides a stronger or more stable stimulus of constitutive *myc* expression then retroviral insertion, as also indicated by the evidence concerning the frequency of chromosome duplication in the former, but not the latter system. As already mentioned, the R-*myc*-, but not the G-*myc*-carrying chromosome 15 tends to duplicate during murine leukaemogenesis. The Ig/*myc* translocation-carrying chromosomes show no similar tendency. With the exception of a single IgL/*myc*-carrying MPC [4] Ig/*myc* translocation, chromosomes were not found to duplicate in any of the three tumours where they regularly occur, i.e. MPC (mouse plasmacytoma), BL (human Burkitt lymphoma) and RIC (rat immunocytoma).

Duplication or hypersomy of the R-*myc*- and loss of the G-*myc*-carrying chromosome in KT-10 suggest a competition between the normal and insertionally activated c-*myc* gene. Both G-*myc* and R-*myc* produce normal proteins but their sensitivity to regulation may differ. It is well known that G-*myc* is governed by multiple regulatory mechanisms in the normal cell dependent on the cell cycle, the differentiation program, the rate of proliferation, and probably other, phenotype related factors. The constitutive activation of R-*myc* by a retroviral enhancer or by juxtaposed immunoglobulin sequences interferes with the normal regulability of the gene.

It is conceivable that the simultaneous presence of a constitutively expressed and a normally regulated *myc* gene may handicap the growing tumour cell, compared to the exclusive presence of the constitutively activated, deregulated gene. If so, the regular maintenance of G-*myc* in the Ig/*myc* translocation-carrying tumours, i.e. lack of a similar selective advantage, may be related to the widely documented finding that such tumours express only the translocated but not the normal *myc* allele [32].

The repeatedly observed hypersomy of the R-*myc*-carrying chromosomes and the concomitant loss of the G-*myc* chromosome from tumours with retrovirally activated *myc* genes suggests the interaction with cellular programs. The *myc* protein may be involved in many as yet unknown programming mechanisms of the cell, as also suggested by the recent discovery on the connection between illegitimate *myc* expression and apoptosis [35].

1. Klein G. The role of gene dosage and genetic transpositions in carcinogenesis. *Nature* 1981, **294**, 313–318.
2. Klein G. The approaching era of tumor suppressor genes. *Science* 1987, **238**, 1539–1545.
3. Quint W, Boelens W, Van Wezenbeek P, *et al.* Generation of AKR mink cell focus-forming virus: nucleotide sequence of the 3′ end of a somatically acquired AKR-MCF. *Virology* 1984, **50**, 432–438.
4. Potter M, Wiener F. Plasmacytomagenesis in mice: model of neoplasmic development dependent upon chromosomal translocations. *Carcinogenesis* 1992, **13**, 1681–1697.
5. Spira J, Wiener F, Babonits M, Gamble J, Miller J, Klein G. The role of chromosome 15 in murine leukemogenesis I. Contrasting behaviour of the tumor vs. normal parent derived chromosome no. 15 in somatic hybrids of varying tumorigenicity. *Int J Cancer* 1981, **28**, 785–789.
6. Cory S, Adas JM, Gerondakis SD, *et al.* Fusion of DNA region to murine immunoglobulin heavy chain locus corresponds to plasmacytoma-associated chromosome translocation. *EMBO J* 1983, **2**, 213–216.
7. Wirschubsky Z, Wiener F, Spira J, Sümegi J, Klein G. Triplication of one chromosome no. 15 with altered c-*myc* containing *Eco*RI fragment and elimination of the normal homologue in a T-cell lymphoma line of AKR origin (TIKAUT). *Int J Cancer* 1984, **33**, 477–481.
8. Corcoran LM, Adams JM, Dunn AR, Cory S. Murine T lymphomas in which the cellular *myc* oncogene has been activated by retroviral insertion. *EMBO J* 1984, **37**, 113–122.
9. Wirschubsky Z, Tsichlis P, Klein G, Sümegi J. Rearrangement of c-*myc*, *pim*-1 and *Mlvi*.1 and trisomy of chromosome 15 in MCF- and Moloney-MuLV-induced murine T-cell leukemias. *Int J Cancer* 1986, **38**, 379–745.
10. Uno M, Wirschubsky Z, Babonits M, Wiener F, Sümegi J, Klein G. The role of chromosome 15 in murine leukemogenesis. II. Relationship between tumorigenicity and the dosage of lymphoma vs. normal parent derived chromosome 15 in somatic cell hybrids. *Int J Cancer* 1987, **40**, 540–549.
11. Graham M, Adams JM, Cory S. Murine T lymphoma with retroviral inserts in the chromosome 15 locus for plasmacytoma variant translocation. *Nature* 1985, **314**, 740–743.
12. Uno M, Wirschubsky Z, Wiener F, Klein G. Relationship between tumorigenicity and the dosage of lymphoma- vs. normal parent derived chromosome 15 in somatic cell hybrids between lymphoma cells rearranged *pvt*-1 gene and normal cells. *Int J Cancer* 1989, **44**, 353–360.
13. Wiener F, Babonits M, Bregula U, *et al.* High resolution banding analysis of the involvement of strain BALB/c and AKR derived chromosomes no. 15 in plasmacytoma specific translocations. *J Exp Med* 1984, **159**, 276–291.
14. Léonard A, DeKnudt GH. 6 new markers for chromosome studies in the mouse. *Nature* 1967, **214**, 504–507.
15. Carter TC, Lyon MF, Phillips RJS. Gene-tagged chromosome translocations in eleven stocks of mice. *J Genet* 1955, **53**, 154–166.
16. Schibler MJ, Barlow SB, Cabral F. Elimination of permeability mutants from selections for drug resistance in mammalian cells. *FASEB J* 1989, **3**, 163–168.
17. Stetten G, Latt SA, Davidson RL. 33258 Hoechst enhancement

of the photosensitivity of bromodeoxyuridine substituted cells. *Somatic Cell Mol Genet* 1976, 2, 285–290.
18. Kuzumaki N, More IAR, Cochran AJ, Klein G. Thirteen new mammary tumor cell lines from different mouse strains. *Eur J Cancer Clin Oncol* 1980, **16**, 1181–1192.
19. Seabright M. A rapid banding technique for human chromosomes. *Lancet* 1971, **ii**, 971–972.
20. Summer AT. A simple technique for demonstrating centromeric heterochromatin. *Exp Cell Res* 1972, **75**, 304–306.
21. Ronne M. Methotrexate-leucovorin synchronisation of bone marrow culture. Induction of high-resolution R- and G-banding. *Anticancer Res* 1985, 5, 171–171.
22. Committee on Standardized Genetic Nomenclature for Mice. Standard karyotype of the mouse, Mus musculus. *J Hered* 1972, **63**, 69–71. Also, Lyon MF and Searle AG, eds. *Genetic Variants and Strains of the Laboratory Mouse*. Oxford, Oxford Univ Press, 1989, 574–581.
23. Wong AKC, Rattner JB. Sequence organisation and cytological localization of the minor sattelite of mouse. *Nucleic Acids Res* 1988, **16**, 11645–11661.
24. Pinkel D, Gray JW, Trask B, Engh G, Fuscoe J. Cytogenetic analysis by *in situ* hybridization with fluorescently labeled nucleic acid probes. *Cold Spring Harb Symp Quant Biol* 1986, **51**, 151–157.
25. Stanton LW, Watt R, Marcu KB. Translocation breakage and truncated transcripts of c-*myc* oncogene in murine plasmacytomas. *Nature* 1983, **303**, 401–406.
26. Cory S, Graham M, Webb E, Corcoran L, Adams JM. Variant (6;15) translocations in murine plasmacytomas involve a chromosome 15 locus at least 72 kb from the c-*myc* oncogene. *EMBO J* 1985, **4**, 675–681.
27. Axelson H, Kumar Panda Ch, Silva S, *et al.* A new variant (15;16) translocation in mouse plasmacytoma leads to juxtaposition of c-*myc* and Ig-lambda. *Oncogene* 1991, **6**. 2263–2270.
28. Carson WU. A linkage map of the mouse immunoglobulin lambda light chain locus. 1989, **29**, 173–179.
29. Hara H, Sam M, Maki RA, Wu GE, Paige CJ. Characterisation of a 70Z/3 pre-B cell derived macrophage clone. Differential expression of *Hox* family genes. *Int Immunol* 1990, **2**, 691–696.
30. Klinken SP. Transformation of hemopoietic cells by *raf* and *myc* oncogenes: a new perspective on lineage commitment. *Cancer Cells* 1991, **3**, 373–382.
31. Nusse R. The activation of cellular oncogenes by retroviral insertion. *TIG* 1986, **9**, 244–247.
32. Cory S. Activation of cellular oncogenes in hemopoietic cells by chromosome translocation, *Adv Cancer Res* 1986, **47**, 189–234.
33. Herbst EW, Gropp A, Tietgen C. Chromosome rearrangements involved in the origin of trisomy 15 in spontaneous leukemia of AKR mice. *Int J Cancer* 1981, **28**, 805–810.
34. Banerjee M, Wiener F, Spira J,Babonits M, Nilsson M-G, Sümegi J, Klein G. Mapping of the c-*myc*, *pvt*-1 and immunoglobulin kappa genes in relation to the mouse plasmacytoma-associated variant (6;15) translocation breakpoint. *EMBO J* 1985, **4**, 3183–3188.
35. Evan GI, Wyllie AH, Gilbert CS, *et al.* Inductionof apoptosis in fibroblasts by c-*myc* protein. *Cell* 1992, **69**, 119–128.

Acknowledgements—This work was supported by Public Health Service grant 5R01CA14054 from NIH. S.I. was a recipient of a Cancer Research Institute/Concern Foundation for Cancer Research grant. We thank S. Gordon for F 4/80 antibody. The technical assistance of M.-L. Solberg, M. Hagelin, K. Benedek, M. Hedenskog and A. Karlsson is acknowledged.

Pergamon

European Journal of Cancer Vol. 30A, No. 7, pp. 1002–1007, 1994
Elsevier Science Ltd
Printed in Great Britain
0959-8049/94 $7.00+0.00

0959-8049(94)E0177-6

Expression of P-Glycoprotein and *In vitro* or *In vivo* Resistance to Doxorubicin and Cisplatin In Breast and Ovarian Cancers

S. Veneroni, N. Zaffaroni, M.G. Daidone, E. Benini, R. Villa and R. Silvestrini

The expression of P-glycoprotein (P-gp) was studied by immunocytohistochemistry, using the C219 monoclonal antibody, in 39 locally advanced breast cancers and 20 ovarian cancers from previously untreated patients. P-gp was expressed in 46 and 35% of breast and ovarian tumours, respectively. A significant association was observed in both tumour types between P-gp expression and *in vitro* resistance to doxorubicin. We also observed a higher clinical response rate to doxorubicin ± vincristine in patients with breast cancers not expressing P-gp. Conversely, no correlation was found between P-gp expression and *in vitro* resistance to cisplatin or *in vivo* response to cisplatin ± cyclophosphamide treatment in ovarian cancers. Our results support the relevance of P-gp expression as a specific indicator of resistance to certain drugs, such as doxorubicin and vincrinstine, involved in the phenomenon of multidrug resistance in breast and ovarian cancer cells.

Key words: *P*-glycoprotein, multidrug resistance, doxorubicin, breast cancer, ovarian cancer, immunocytohistochemistry, chemosensitivity assays
Eur J Cancer, Vol. 30A, No. 7, pp. 1002–1007, 1994

INTRODUCTION

INTRINSIC OR acquired resistance to various chemotherapeutic agents is a major problem in cancer treatment. Among the different markers, P-glycoprotein (P-gp) is the most consistently described as an indicator of multidrug resistance (MDR) in a wide variety of animal and human tumour cell lines [1–9]. In fact, an increased P-gp level has been reported to be associated with MDR amplification or overexpression in experimental systems [1]. More recently, significantly raised P-gp levels have been detected in untreated and previously treated human